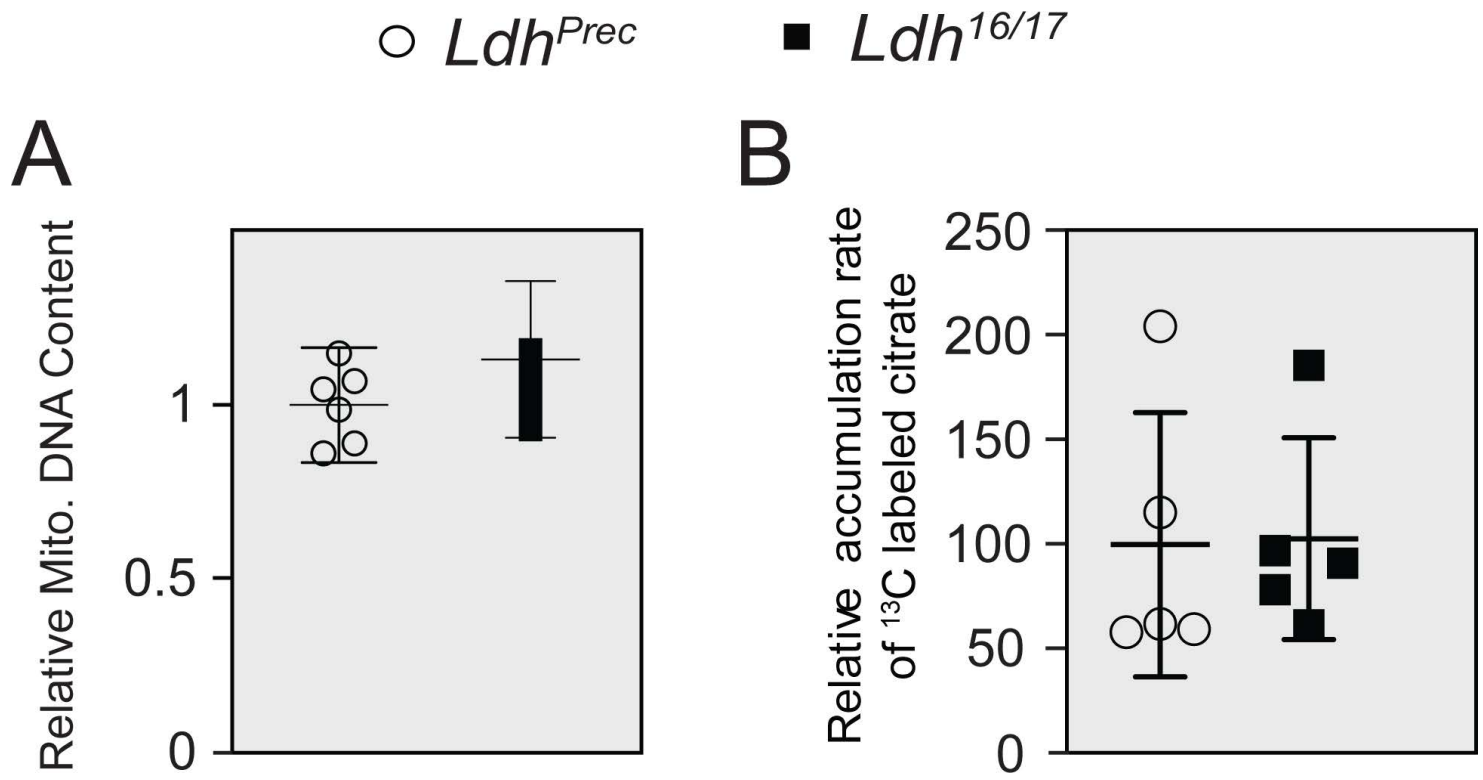

Figure S1. Mitochondrial abundance and citrate synthesis are unaffected by *Ldh* mutations. (A) The relative abundance of mitochondrial DNA is similar in *Ldh*^{prec} controls and *Ldh*$^{16/17}$ mutants. Ratio is based on the abundance of *mt::CoI* copy number relative to *Rpl32* copy number. *n* = 6. (B) The relative metabolic flux rates from $^{13}C_6$-glucose into citrate was measured in *Ldh*^{prec} controls and *Ldh*$^{16/17}$ mutants. *n* = 5. (A,B) Error bars represent mean +/- one standard deviation.

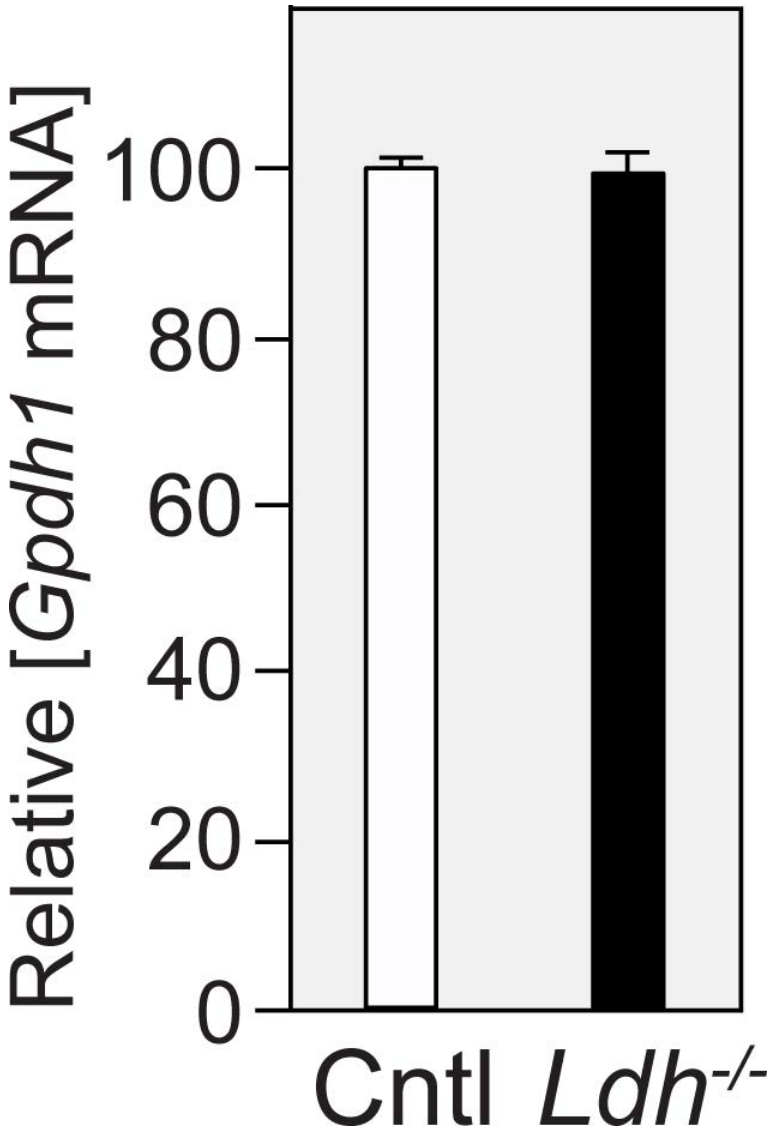

Figure S2. *Ldh* mutants do not exhibit up-regulation of *Gpdh1* gene expression. The abundance of *Gpdh1* mRNA in mid-L2 larvae were measured relative to *rp49* mRNA in Ldh^{prec} controls and $Ldh^{16/17}$ mutants. n=3 independent biological samples. Error bars represent one standard deviation.

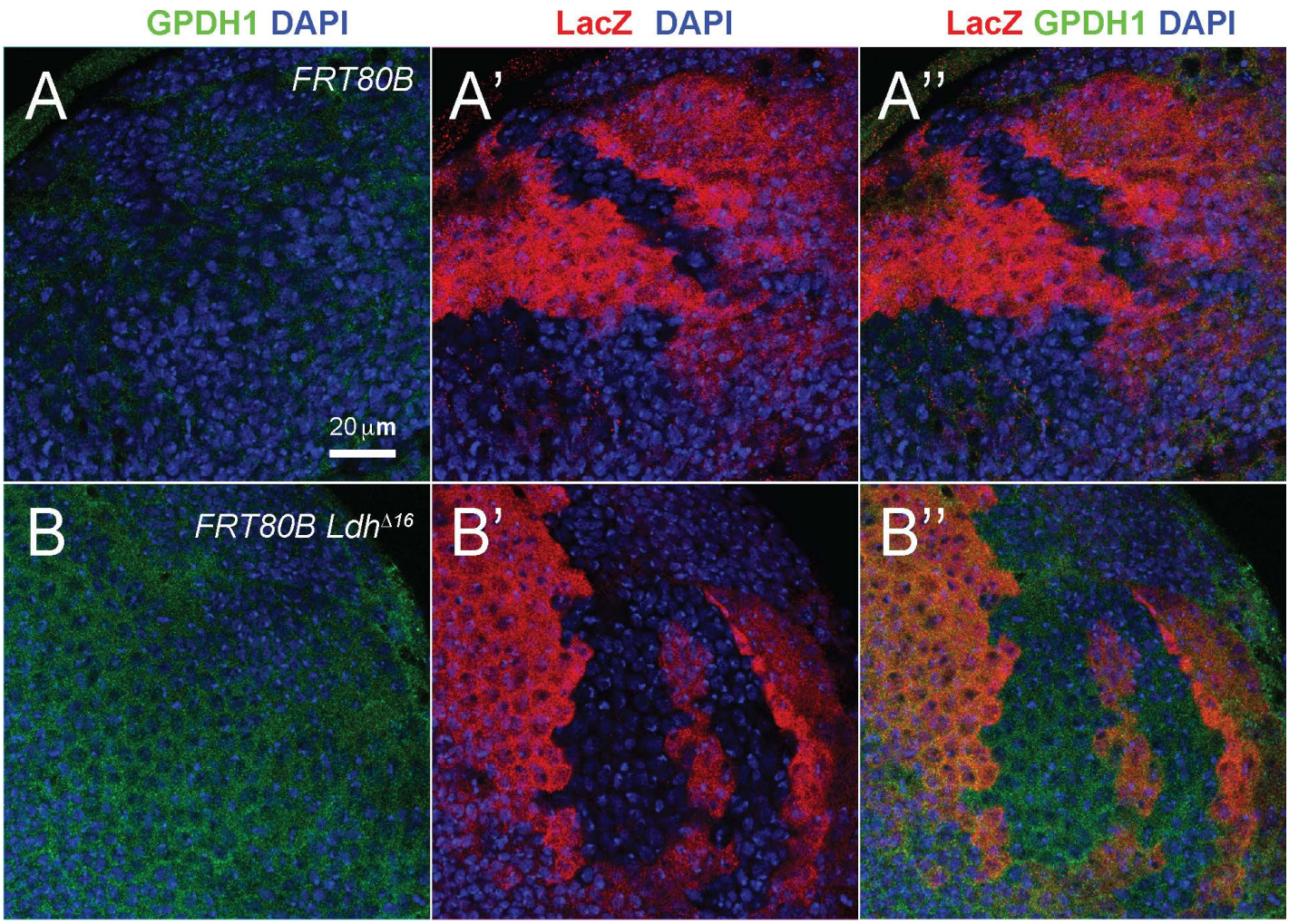

Figure S3. GPDH1 enzyme expression is not increased in *Ldh* mutant cells. CNS clones were generated in either (A) control (*FRT80B*) or (B) Ldh^{16} heterozygous (*FRT80B* Ldh^{16}) background. Tissues were stained with anti-GPDH1, anti-LacZ, and DAPI. (A' and B') Wild-type cells are indicated by increased LacZ staining. (B') Homozygous Ldh^{16} cells lack LacZ staining. (B and B'') The intensity of anti-GPDH1 staining is similar in both wild-type and mutant cells. The scale bar in (A) applies to all panels.

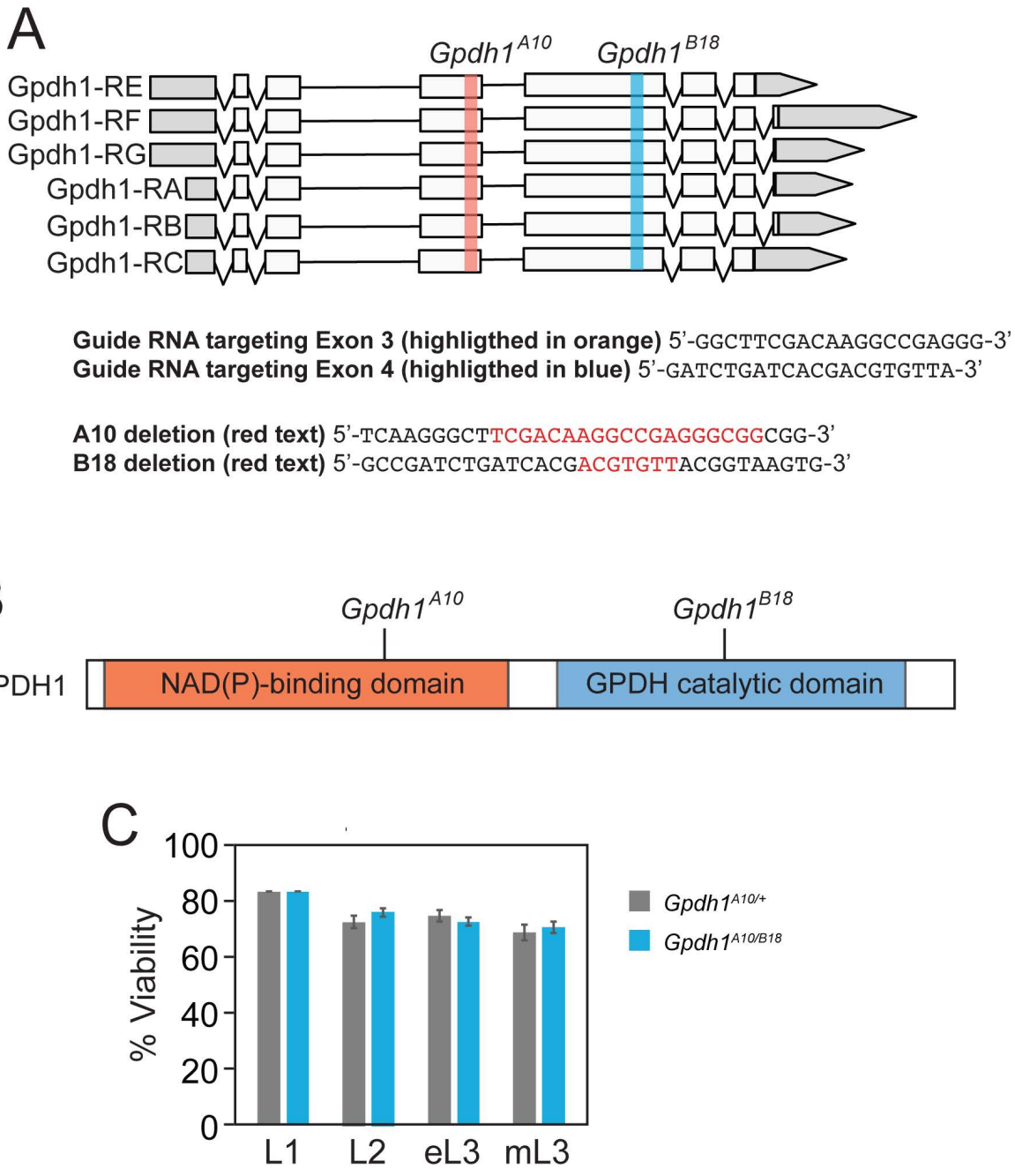

Figure S4. Generation of *Gpdh1* mutants. (A) A schematic diagram illustrating the *Gpdh1* locus, sequences targeted by guide RNA constructs, and sequence deleted by the $Gpdh1^{A10}$ and $Gpdh1^{B18}$ mutations, respectively. The guide RNA targeting exon 3 was used to generate $Gpdh1^{A10}$ and the guide RNA targeting exon 4 was used to generate $Gpdh1^{B18}$. Deleted bases are highlighted in red. (B) A schematic diagram illustrating the location of the $Gpdh1^{A10}$ and $Gpdh1^{B18}$ mutations within the GPDH1 protein. (C) $Gpdh1^{A10/+}$, and $Gpdh1^{A10/B18}$ mutants were analyzed for larval viability. Bars represent the percent of animals that survived from the previous developmental stage until the stage noted on the x-axis. Error bars represent standard deviation. n>100 larvae per timepoint.

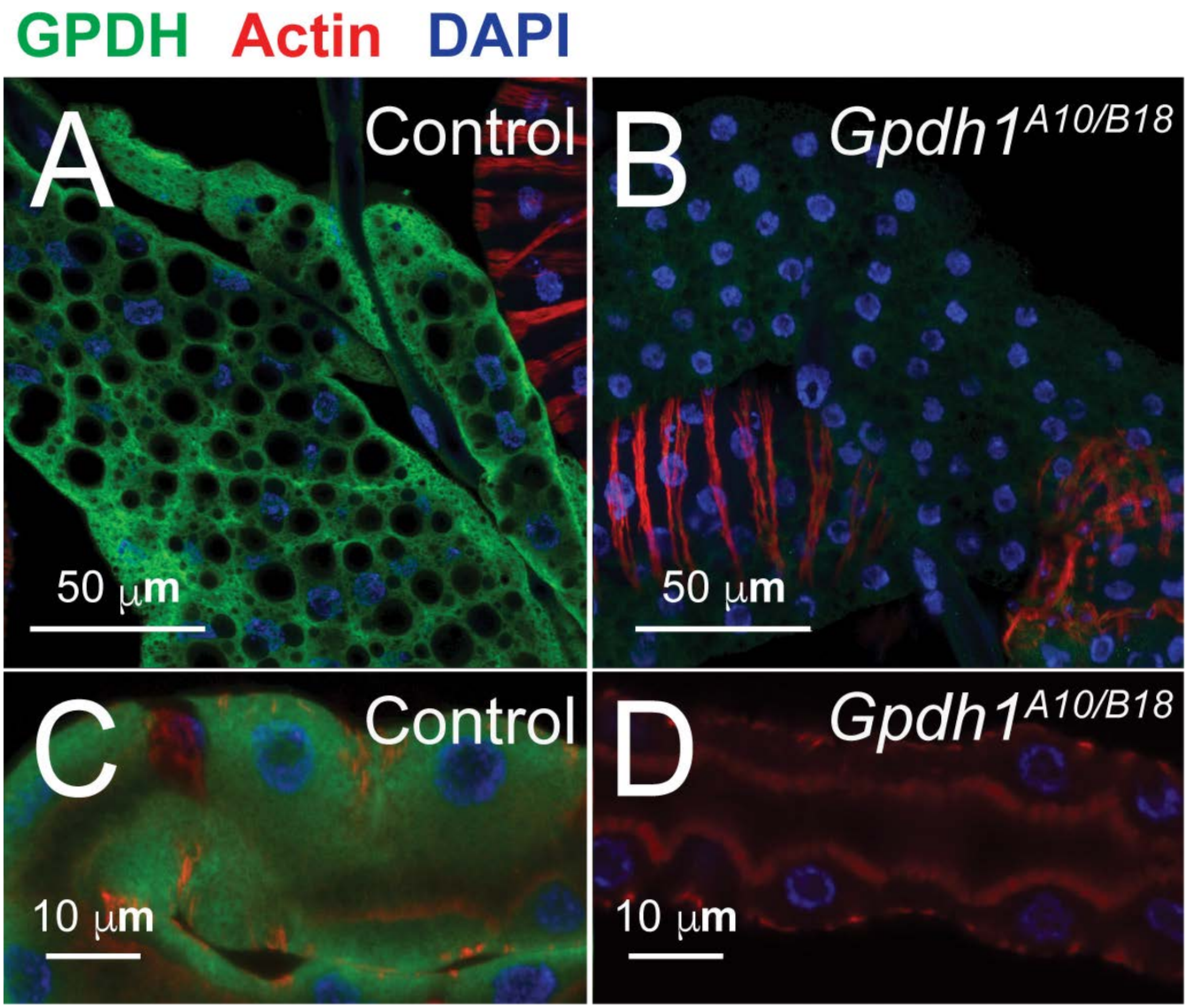

Figure S5. *Gpdh1* mutants exhibit a significant decrease in Gpdh1 enzyme levels. w^{1118} controls and w^{1118}; $Gpdh^{A10/B18}$ mutants were stained with an anti-GPDH1 antibody, phalloidin, and DAPI. (A-B) Representative images of stained fat bodies from (A) w^{1118} controls and (B) w^{1118}; $Gpdh^{A10/B18}$ mutants. (C-D) Representative images of stained Malpighian tubules from (C) w^{1118} controls and (D) w^{1118}; $Gpdh^{A10/B18}$ mutants.

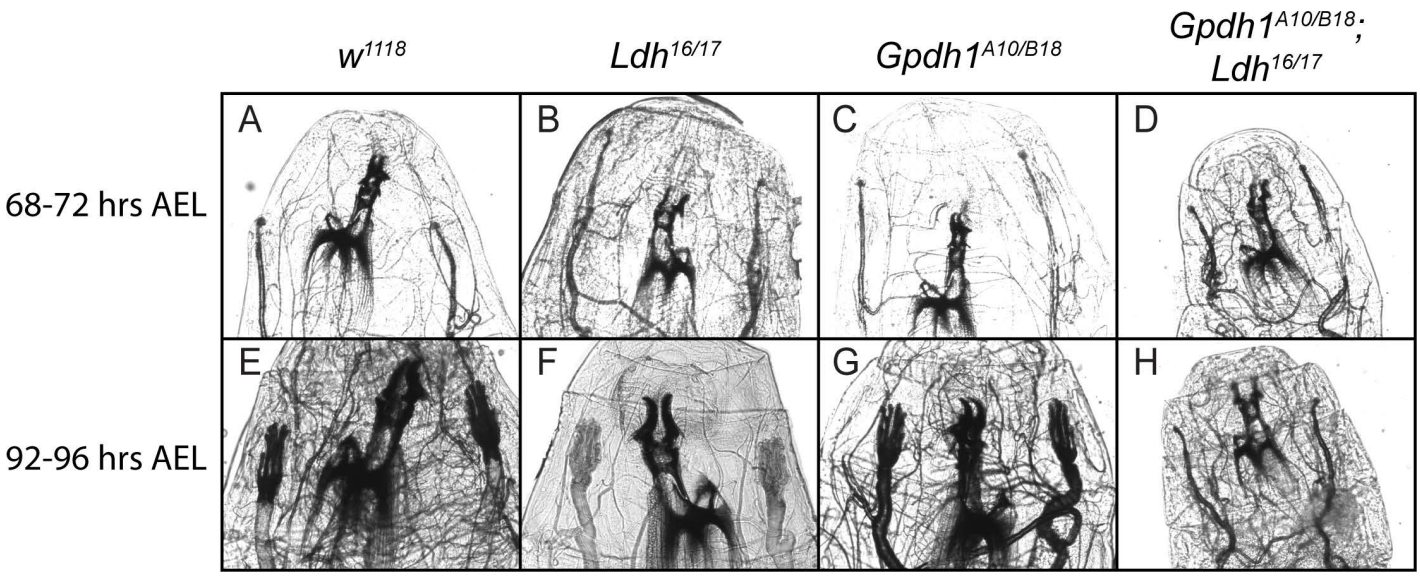

Figure S6. Developmental Staging of *Gpdh*$^{A10/B18}$; *Ldh*$^{16/17}$ double mutant larvae. The mouth hooks and anterior spiracles of *w*^{1118}, *Ldh*$^{16/17}$, *Gpdh1*$^{A10/B18}$, and *Gpdh1*$^{A10/B18}$; *Ldh*$^{16/17}$ double mutant larvae that were imaged at either (A-D) 68-72 hours after egg-laying or (E-H) 92-96 hours after egg-laying. (A-D) For all genotypes, larvae collected 68-72 hours after egg-laying exhibited L2 morphology. (E-H) *w*^{1118}, *Ldh*$^{16/17}$, and *Gpdh1*$^{A10/B18}$ larvae collected 92-96 hours after egg-laying exhibited L3 morphology while *Gpdh1*$^{A10/B18}$; *Ldh*$^{16/17}$ double mutants were still L2s.

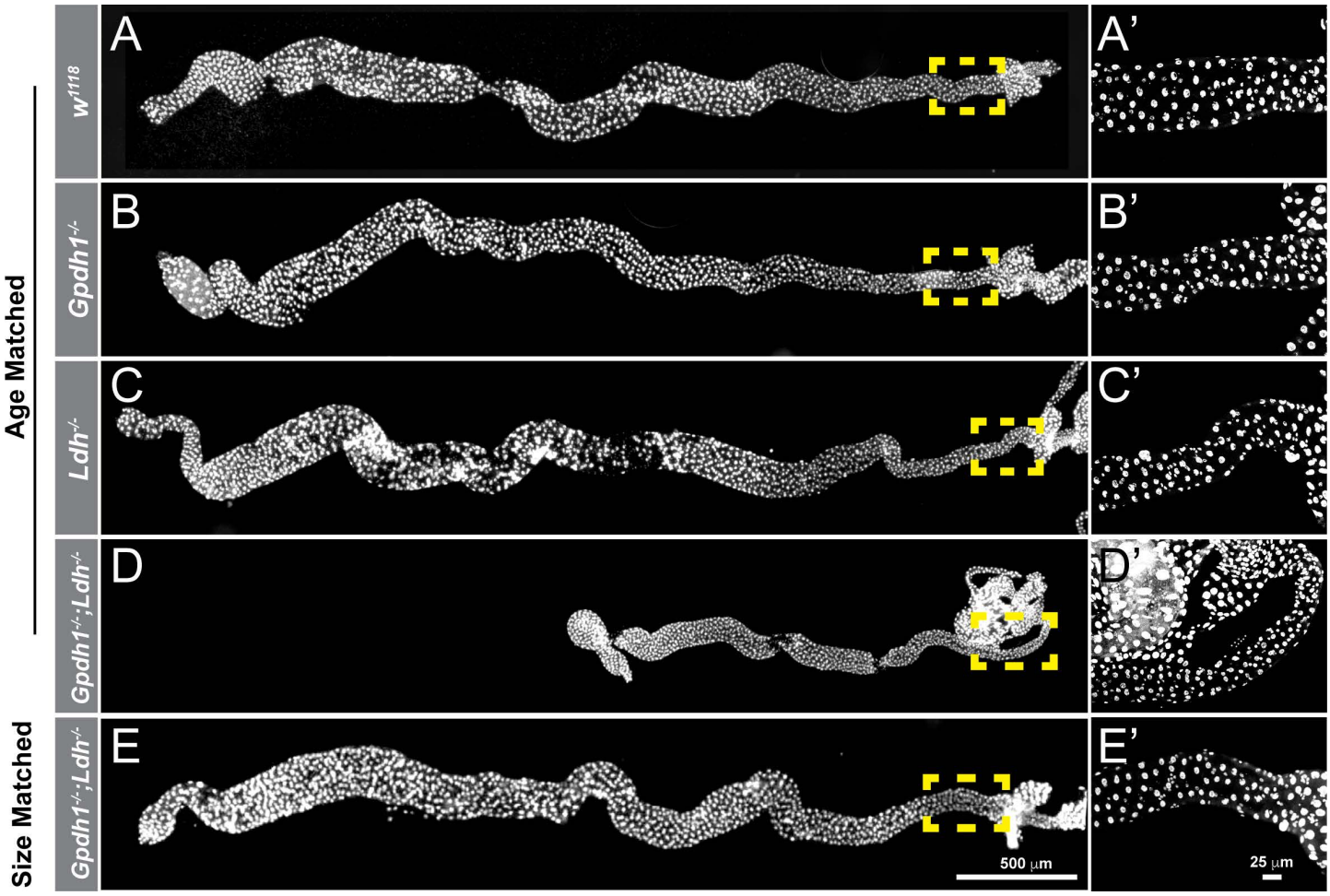

Figure S7. The intestine of *Gpdh*$^{A10/B18}$; *Ldh*$^{16/17}$ double mutant larvae exhibit growth defects (A-E) L2 larval posterior midguts (PMGs) stained for DAPI (gray) from (A) *w*^{1118} controls, (B) *Gpdh1*$^{A10/B18}$ mutants, (C) *Ldh*$^{16/17}$ mutants, (D) age-matched *Gpdh1*$^{A10/B18}$; *Ldh*$^{16/17}$ double mutants, and (E) size-matched *Gpdh1*$^{A10/B18}$; *Ldh*$^{16/17}$ double mutants. (A'-E') Magnified images of the outlined regions in A-E. The scale bars in (E) and (E') apply to (A-E) and (A'-E'), respectively.

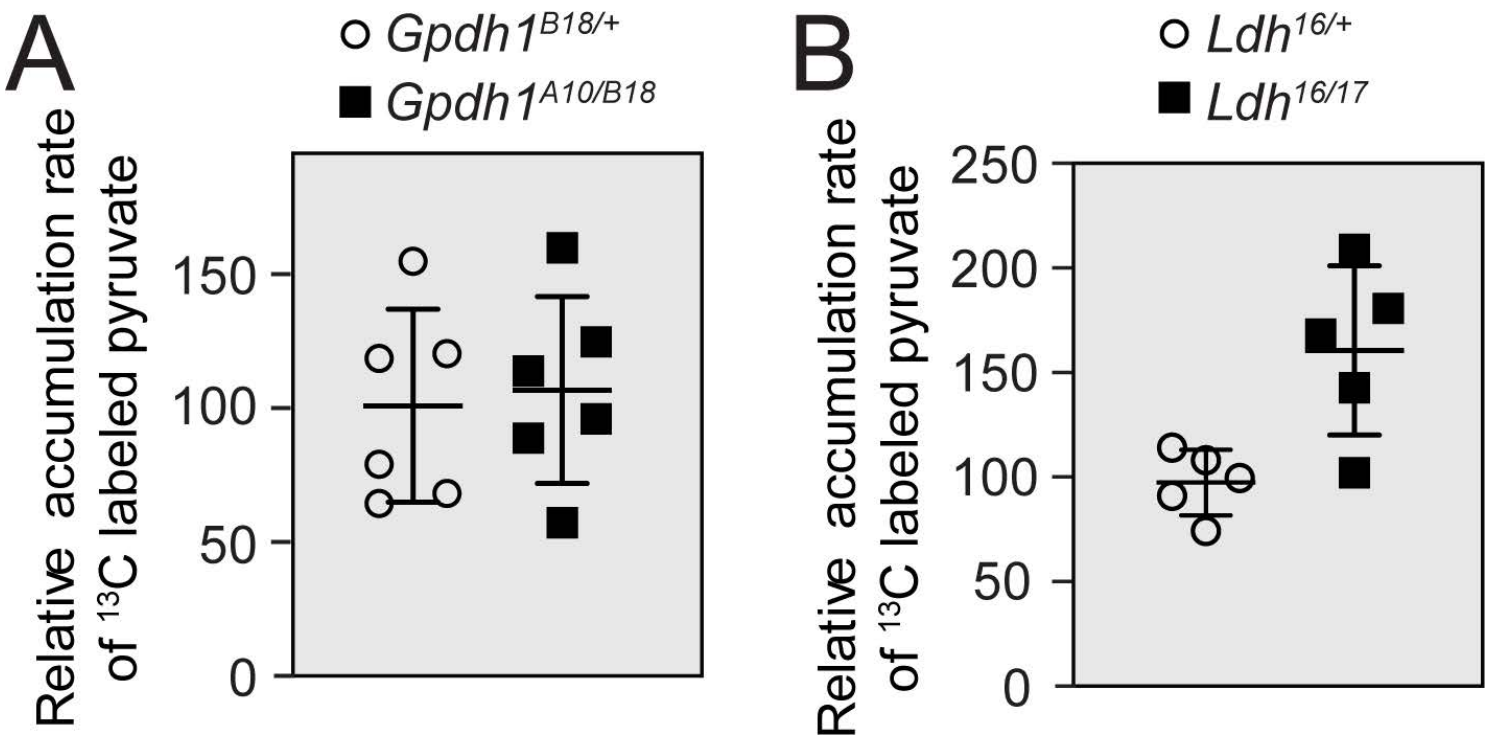

Figure S8. *Gpdh1* and *Ldh* mutants exhibit normal rates of pyruvate accumulation. The relative metabolic flux rate from $^{13}C_6$-glucose into pyruvate was measured in (A) *Gpdh1*$^{A10/B18}$ mutant L2 larvae compared to *Gpdh1*$^{B18/+}$ controls and (B) *Ldh*$^{16/17}$ mutant L2 larvae compared to *Ldh*$^{16/+}$ controls. For all panels, error bars represent one standard deviation. (A) n=6 biological replicates. (B) n=5 biological replicates. The increased abundance observed in (B) is not significant.

Table S1. Summary of LC-MS analysis of *Ldh* mutants and precise excision controls. n= number of independent samples analyzed per genotype in the experiments. Each sample contained 100 mid-L2 larvae.

Click here to Download Table S1

Table S2. Absolute abundance of TAG, glycogen, and trehalose in *Ldh* mutants and precise excision controls. Data represented in Figure 1C.

Click here to Download Table S2

Table S3. Summary of GC-MS metabolomic analyses (*Ldh* mutants vs Precise excision controls). Individual trials consist of 6 independent samples per genotype. Each sample contains 25 mid-second instar larvae. Highlighted values indicate a minimum 2-fold change and a p-value of 0.01. Data for all samples are available in the Supplemental Results.

Click here to Download Table S3

Table S4. GC-MS analysis of *Ldh* mutants and precise excision controls (Trial 1).
All values normalized to sample mass and a d-4-succinic acid standard. n=6 samples per genotype; 25 mid-L2 larvae per sample.

Click here to Download Table S4

Table S5. GC-MS analysis of *Ldh* mutants and precise excision controls (Trial 2).
All values normalized to sample mass and a d-4-succinic acid standard. n=6 samples per genotype; 25 mid-L2 larvae per sample.

Click here to Download Table S5

Table S6. GC-MS analysis of *Ldh* mutants and precise excision controls (Trial 3).
All values normalized to sample mass and a d-4-succinic acid standard. n=6 samples per genotype; 25 mid-L2 larvae per sample.

Click here to Download Table S6

Table S7. GC-MS analysis of *Ldh* mutants and precise excision controls (Trial 4). All values normalized to sample mass and a d-4-succinic acid standard. n=6 samples per genotype; 25 mid-L2 larvae per sample.

Click here to Download Table S7

Table S8. GC-MS analysis of *Gpdh1[A10/+]* heterozygous controls and *Gpdh1[A10/B18]* mutants. All values normalized to sample mass and a d-4-succinic acid standard. n=6 samples per genotype; 25 mid-L2 larvae per sample.

Click here to Download Table S8

Table S9. GC-MS analysis of *Gpdh1[A10/+]; Ldh[16/+]* heterozygous controls and *Gpdh1[A10/B18]; Ldh[16/17]* mutants. All values normalized to sample mass and a d-4-succinic acid standard. n=6 samples per genotype; 25 mid-L2 larvae per sample.

Click here to Download Table S9